

Nonrelativistic electron bunch train for coherently enhanced terahertz radiation sources

Yuelin Li^{a)} and Kwang-Je Kim

Accelerator Systems Division and Argonne Accelerator Institute, Argonne National Laboratory, Argonne, Illinois 60439, USA

(Received 8 October 2007; accepted 4 December 2007; published online 2 January 2008)

We propose to generate a train of prebunched electron beams for producing coherently enhanced Smith-Purcell radiation [S. J. Smith and E. M. Purcell, *Phys. Rev.* **92**, 1069 (1953)] in the terahertz wavelength range. In this scheme, a train of picosecond laser pulses is produced to drive a photoemission gun to generate a train of 50 keV electron pulses. The parameters are chosen so that the space-charge effect does not destroy the pulse time structure. Smith-Purcell radiation from the electron pulse train is enhanced due both to the short length of the individual electron bunch and to the repetitive structure of the beam. Example systems producing coherent terahertz power at about 1 mW are described. © 2008 American Institute of Physics. [DOI: 10.1063/1.2828337]

Demand for terahertz radiation is increasing in various areas of science and technology, such as material characterization, chemical and biological analyses, and a variety of imaging applications.¹ Among various terahertz sources, laser-based techniques using a difference-frequency mixing scheme are more compact² while electron beam based sources in large accelerator installations provide higher power.³ In this note, we discuss an electron-beam-based source that is also compact.

The radiation from an electron bunch has two components, the coherent component and the incoherent component,

$$\frac{dI}{d\omega} = \left(\frac{dE}{d\omega}\right)^2 (N + N^2\sigma_{\text{coh}}), \quad (1)$$

where $dE/d\omega$ and $dI/d\omega$ are, respectively, the radiation field from individual electrons and spectral intensity from the bunch, and N is the total number of particles. Here, $\sigma_{\text{coh}} = [\int S(r)\cos(kr)dr / \int S(r)dr]^2$ is the coherence factor,⁴ with S being the particle distribution and $k = \omega/c$. In the time domain, this is effectively the normalized Fourier intensity of the longitudinal beam profile, $\sigma_{\text{coh}} = [\int S(t)\cos(\omega t)dt / \int S(t)dt]^2$. In Fig. 1(a), σ_{coh} is evaluated for two different particle distributions: ellipsoidal and Gaussian. Obviously, to harvest the coherent enhancement, i.e., the N^2 effect, a high bunch charge and an rms bunch size much smaller than the radiation wavelength are desired.

However, at high bunch charges, the space charge effect can become large, thus resulting in the destruction of the short bunch structure during the beam transport. This effect is especially prominent for nonrelativistic beams and crucial for many applications such as ultrafast electron diffraction experiments, and has been analyzed by several authors.⁵⁻⁷ Here, we use the formula in Ref. 5 that describes the evolution of uniform ellipsoidal beams and in excellent agreement with particle simulation.⁵ The free-space bunch evolution is shown in Fig. 1(b), where we show the rms beam length $\sigma_z/\beta\lambda$ (note that for an ellipsoidal beam $\sigma_z = Z/\sqrt{5} \approx Z/2$, where Z is the half bunch length) as a function of the propagation distance. Here, $\lambda = 652 \mu\text{m}$ is the radiation wave-

length, and $\beta = 0.41$ is the beam velocity normalized to the speed of light, corresponding to a beam energy of 50 keV. The bunches start with the same transverse and longitudinal sizes. Clearly, with these parameters, a single bunch with a charge of more than a few femtocoulombs can be hard to maintain, and the coherence factor [see Fig. 1(c)], thus the radiation efficiency, drops very quickly. Taking the example in Fig. 1(c) at 3 cm, for $Q = 2$ fC, $\sigma_{\text{coh}} = 0.4$, thus $N^2\sigma_{\text{coh}} = 6 \times 10^7$. Increasing Q to 20 fC reduces σ_{coh} to 10^{-4} , thus $N^2\sigma_{\text{coh}} = 1.6 \times 10^5$, a reduction in power of more than two orders of magnitude.

The space charge effect can be significantly reduced if the charge is distributed into many bunches, and each bunch can be well preserved. It follows that for electron beams with N_b repetitive temporal structure of $S(t - n\tau_b)$, $n = 1, \dots, N_b$, the overall coherence factor is

$$\Sigma_{\text{coh}} = \sigma_{\text{coh}} \frac{1}{N_b^2} \left(\sin \frac{N_b \tau_b \omega}{2} \bigg/ \sin \frac{\tau_b \omega}{2} \right)^2, \quad (2)$$

where $\tau_b = 1/\beta c$ is the bunch spacing and σ_{coh} is the single bunch coherence factor. Although the radiation power from each bunch is reduced by a factor of N_b^2 , within a bandwidth of $1/N_b$ at $\omega = 2\pi/\tau_b$, it is enhanced by a factor of N_b^2 , thus one has $\Sigma_{\text{coh}} = \sigma_{\text{coh}}$. For example, in Figs. 1(b) and 1(c), by distributing 20 fC into 20 bunches, the bunch structure is well maintained up to a propagation distance of a few centimeters and so is the coherence factor $\Sigma_{\text{coh}} = 0.6$ at $\lambda = \tau_b c$, thus we have $N^2\sigma_{\text{coh}} = 9 \times 10^9$, almost five orders of magni-

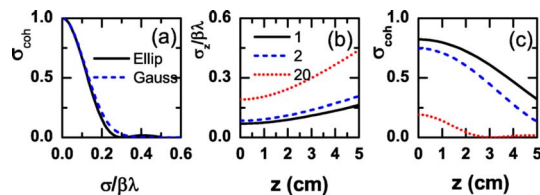


FIG. 1. (Color online) (a) One dimensional coherence factor for different bunch geometry as a function of the rms bunch length normalized to the radiation wavelength λ , here β is the normalized bunch speed. (b) The beam rms length and (c) evolution of the bunch coherence factor as a function of the bunch propagation distance for bunch charges of 1, 2, and 20 fC at $\lambda = 646 \mu\text{m}$ (0.46 THz).

^{a)}Electronic mail: ylli@aps.anl.gov.

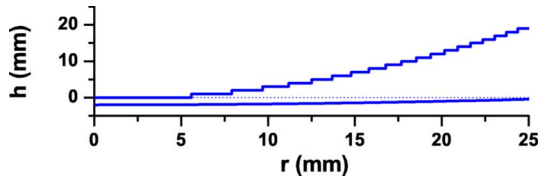


FIG. 2. (Color online) Radial profile of an echelon lens that generates a pulse train from a single laser pulse at the focus.

tude enhancement over the single 20 fC bunch case at the same wavelength.

Enhancement of radiation in a Smith-Purcell radiation experiment^{8,9} from a prebunched beam was observed with 15 MeV electron beams produced by a 17 GHz radio frequency linear accelerator.¹⁰ In this experiment, the high beam energy and larger bunch separation help to preserve the bunch structure. Bunching of electron beam can also be accomplished in a Smith-Purcell backward wave oscillator.^{11,12} However, the system requires a high quality electron beam not readily available and may be very difficult to maintain.¹²

Here, we propose a scheme to generate a train of non-relativistic electron bunches suitable for efficient, coherently enhanced Smith-Purcell radiation generation. The bunch train is initiated from a photocathode by a laser pulse train and subsequently accelerated by a dc field.

For generating a terahertz pulse train, one can use a Michelson interferometer¹³ or birefringence crystals¹⁴ to stack a short pulse, or use the beat between two long laser pulses.¹⁵ Here, we propose a more compact system that consists of a concentric echelon in combination with a focusing lens of which an example is shown in Fig. 2. The echelon consists of a series of concentric flat zones, each having a different thickness, thus displacing the pulses in time at the focus of the lens.

Let a laser pulse of amplitude a_0 with a temporal profile $T(t)$ impinge on the echelon lens. The field at the focus due to the m th zone occupying the radial region $r_m \leq r \leq r_{m+1}$ is given by

$$u_m(t) = 2\pi a_0 T\left(t - \frac{d_m}{v_g}\right) \int_{r_m}^{r_{m+1}} r dr. \quad (3)$$

Here, v_g is the group velocity of light in the lens and d_m is the thickness of the m th zone. Let us choose the zone parameters as follows:

$$d_m = d_0 \pm m\Delta t \left(\frac{1}{v_g} - \frac{1}{c}\right)^{-1},$$

$$r_m = R \sqrt{\frac{m}{M}}, \quad m = 1, 2, \dots, M. \quad (4)$$

Here, d_0 , R , and M are the central thickness of the first zone, the radius of the lens, and the total number of zones, respectively, and Δt is the difference in the travel time in the lens material and the air. The total field at the focus is then a train of pulses spaced at an interval Δt ,

$$u(t) = \frac{\pi a_0 R^2}{M} \sum_{m=1}^M T(t - m\Delta t). \quad (5)$$

To evaluate the performance of this echelon lens, we use a Fourier optics method^{16,17} solving the Helmholtz equation

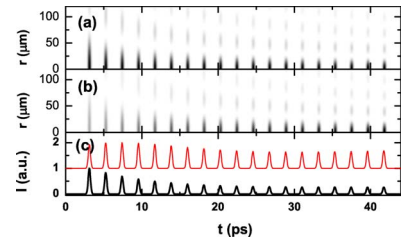


FIG. 3. (Color online) Spatiotemporal intensity distribution of a laser pulse train generated using a $f=1.5$ m echelon lens from a single laser pulse of 0.35 ps, with the zone radius defined (a) by Eq. (4) and (b) by Eq. (6). (c) Comparison of the spatially integrated intensity as a function of time showing a better distribution using Eq. (6) (upper curve) than Eq. (4) (lower curve). The integration is up to a radius of 42 μm .

of the laser field. An example of the calculation is shown in Fig. 3(a), where the spatiotemporal distribution of the laser pulse at the focal plane of $f=1.5$ m and $R=2.5$ cm fused silica lens is depicted. The zone thickness step is 1 mm, giving a pulse spacing of $\Delta t=2.16$ ps. With $M=20$, a train of 19 pulses is generated. The input laser pulse is a transform-limited Gaussian pulse with a FWHM of 0.35 ps at 249 nm.

It is found that dispersion effects are negligible as long as the pulse duration is longer than 20 fs. However, the diffraction due to the phase discontinuity at the zone boundaries gives a series of diffraction structures; this in turn modifies the radially integrated energy distribution along the train, as shown in Fig. 3(c) for a radius of 42 μm . To correct this, the radius sequence is modified as

$$r_m = R \sqrt{\frac{m}{M}} (a + b_1 m + b_2 m^2 + b_3 m^3)^{1/2} \alpha,$$

$$m = 1, 2, \dots, M, \quad (6)$$

where $a=0.35$, $b_1=0.0436$, $b_2=0.00152$, $b_3=0.0000236$, and $\alpha=1.116$ are fitting parameters. The resultant spatiotemporal beam profile is shown in Fig. 3(b), and the radially integrated energy distribution for $r=42$ μm is shown in Fig. 3(c) in comparison with that using Eq. (4). The fitting parameters in Eq. (6) depend on the size of the integration region and the optical setup.

A train of electron bunches with bunch spacing $\tau_b = \Delta t$ will be generated when the laser pulse train is impinged on a photocathode under an accelerating field. To analyze the evolution of such a beam, we started by mapping the laser spatiotemporal intensity distribution into a particle distribution assuming a photocathode with a radius of 42 μm . The beam is accelerated by a dc voltage of 50 kV over a gap of 5 mm, resulting a final $\beta=0.41$. The free-space beam evolution is then simulated using a general purpose particle tracking (GPT) code,¹⁸ which solves the Poisson equation using a nonequidistant mesh. The number of particles used in the simulation is 8000. A thermal energy of 1.1 eV is also included for the initial beam for a realistic emittance evaluation.

Figure 4(a) shows the electrons projected in the x - t plane as seen by a screen at 3 cm from the cathode. The total charge is $Q=20$ fC or 1 fC per bunch. The coherence factor Σ_{coh} as a function of radiation frequency of the beam, depicted in Fig. 4(c), shows a clear peak $\nu=0.46$ THz, with sidebands due to the overall shape of the bunch train. As the beam propagates, bunching starts to deteriorate, as shown in Fig. 4(b), where the current at 1, 3, and 10 cm is compared.

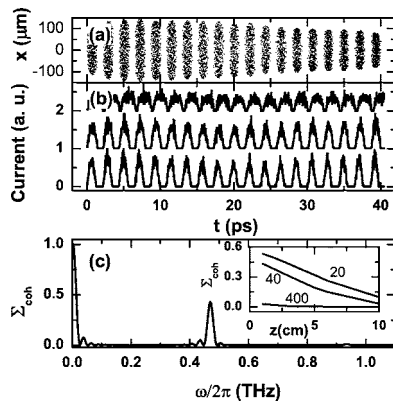


FIG. 4. (a) Particle distribution in the x - t plane as seen by a screen at 3 cm from the photocathode using the laser pulse in Fig. 3. (b) From bottom to top: total current as seen by screens at 1, 3, and 10 cm from the photocathode. (c) Coherence factor, i.e., normalized Fourier spectrum of the beam current at 3 cm, showing a peak at 0.46 THz and its second harmonics. The total charge of the beam is 20 fC unless otherwise indicated. Inset: the coherence factor at 0.46 THz for a total charge of 20, 40, and 400 fC for the train with 19 bunches (from top to bottom).

As expected, the coherence factor at 0.46 THz decreases as the propagation distance and total charge increase, depicted in the inset of Fig. 4(c). In all cases, the final emittance of the beam is very small at about 10^{-3} mm mrad.

An echelon with M much larger than 20 does not appear practical. However, a longer train can be produced by stacking the trains coherently.¹⁹ In the following, we will assume a total number of pulses of 320.

For a bunch charge $Q_b = 2$ fC, the total charge in the train is $Q = 640$ fC. The average current is about $64 \mu\text{A}$ when driven at 100 MHz. Consider Smith-Purcell radiation by passing the beam above a 5 cm grating, centered at about 3 cm from the cathode, with the groove period $\lambda_g = \beta\lambda = 267 \mu\text{m}$, thus the number of grooves is $N_g = 187$. Coherently enhanced terahertz radiation at $\lambda = 648 \mu\text{m}$ will be emitted in the direction normal to the electron beam direction. Using the formula in Refs. 9 and 10, the average radiation power is 0.1 mW in a $1/N_b$ bandwidth, considerable for the terahertz range. In the estimate, we assume that the beam is positioned $60 \mu\text{m}$ (the rms beam size at 3 cm) above the grating and a 100% grating efficiency.

Further simulation and analytical evaluation show that limiting the transverse expansion of the beam by a solenoid has negligible effect on the longitudinal beam evolution for the parameter considered. In this case, the transverse beam size can be maintained at the starting value of about $20 \mu\text{m}$ (rms), and the THz power can be raised to 0.3 mW.

For cathode materials such as copper and magnesium, the response time on the order of a few femtoseconds and the quantum efficiency at 250 nm is between 5×10^{-5} and 5×10^{-4} .^{20,21} With a 10% conversion efficiency from the fundamental to third harmonic, a laser at 800 nm of less than 10 W is enough for producing the required beam current. With higher power, more bunches can be generated and the terahertz power scales as the square of the laser power.

Besides pulse staking from short pulses, a laser pulse train suitable for this application can also be generated using a beat wave between two long-pulse, phase-locked lasers with a slight shift of the central frequencies. Although the beat wave does directly generate well-spaced pulses,¹⁵ steep-

ening of the individual pulse can be achieved during frequency conversion. Much higher radiation power can be expected in such system.¹⁹

The efficiency of such a system is limited by the effective radiation length, during which the beam must maintain its bunching structure. It should be pointed out, though we have limited our discussion here on application in terahertz radiation generation, the scheme is also applicable for generating more tightly spaced bunches in higher gradient injectors, and thus may lead to a direct seeding of short wavelength free-electron lasers. It is also noticed that even after that the bunch structure disappears, a saw-tooth type of energy modulation persists along the beam,¹⁹ making it possible to rebunch via phase space manipulation at a later accelerating stage.

In summary, we show that it is possible to generate non-relativistic bunch trains with a bunch rate in the terahertz regime with a laser-driven compact dc accelerator, providing coherence enhancement for terahertz radiation. In comparison with a device using cw electron beams, the efficiency enhancement is on the order of 10^4 – 10^6 , i.e., the number of the particles in each bunch of the electron and the beam. The experiment can be arranged by placing a grating very close the cathode and may be implemented in a retrofitted electron microscope.^{22,23}

The authors thank K. Harkay for support. This work is supported by the U.S. Department of Energy, Office of Science, Office of Basic Energy Sciences, under Contract No. DE-AC02-06CH11357.

¹B. Ferguson and X. C. Zhang, *Nat. Mater.* **1**, 26 (2002).

²K. Kawase, J. Shikata, K. Imai, and H. Ito, *Appl. Phys. Lett.* **78**, 2819 (2001).

³G. L. Carr, M. C. Martin, W. R. McKinney, K. Jordan, G. R. Neil, and G. P. Williams, *Nature (London)* **420**, 153 (2002).

⁴J. S. Nodvick and D. S. Saxon, *Phys. Rev.* **96**, 180 (1954).

⁵Y. K. Batygin, *Phys. Plasmas* **8**, 3103 (2001).

⁶B. J. Siwick, J. R. Dwyer, R. E. Jordan, and R. J. D. Miller, *J. Appl. Phys.* **92**, 1643 (2002).

⁷A. M. Michalik and J. E. Sipe, *J. Appl. Phys.* **99**, 054908 (2006).

⁸S. J. Smith and E. M. Purcell, *Phys. Rev.* **92**, 1069 (1953).

⁹P. M. van den Berg, *J. Opt. Soc. Am.* **63**, 1588 (1973).

¹⁰S. E. Korbly, A. S. Kesar, J. R. Sirigiri, and R. J. Temkin, *Phys. Rev. Lett.* **94**, 054803 (2005).

¹¹H. L. Andrews and C. A. Brau, *Phys. Rev. ST Accel. Beams* **7**, 070701 (2004).

¹²K.-J. Kim and V. Kumar, *Phys. Rev. ST Accel. Beams* **10**, 080702 (2007).

¹³C. Sider, *Appl. Opt.* **37**, 5302 (1998).

¹⁴B. Dromey, M. Zepf, M. Landreman, K. O'Keeffe, T. Robinson, and S. M. Hooker, *Appl. Opt.* **46**, 5142 (2007).

¹⁵T. Inoue, J. Hiroishi, T. Yagi, and Y. Mimura, *Opt. Lett.* **32**, 1596 (2007).

¹⁶M. Kempe, U. Stamm, B. Wilhelmi, and W. Rudolph, *J. Opt. Soc. Am. B* **9**, 1158 (1992).

¹⁷J. Goodman, *Introduction to Fourier Optics* (McGraw-Hill, New York, 1988).

¹⁸<http://www.pulsar.nl/gpt>

¹⁹Y. Li (unpublished).

²⁰D. H. Dowell, F. K. King, R. E. Kirby, and J. F. Schmerge, *Phys. Rev. ST Accel. Beams* **9**, 063502 (2006).

²¹T. Srinivasan-Rao, I. Ben-Zvi, J. Smedley, X. J. Wang, and M. Woodle, *Proceedings of the Particle Accelerator Conference, 1997* (unpublished), Vol. 97, p. 2790.

²²J. Urata, M. Goldstein, M. F. Kimmitt, A. Naumov, C. Platt, and J. E. Walsh, *Phys. Rev. Lett.* **80**, 516 (1998).

²³O. H. Kapp, Y. E. Sun, K.-J. Kim, and A. V. Crewe, *Rev. Sci. Instrum.* **75**, 4732 (2004).